Global Ecology and Conservation 31 (2021) e01835

Contents lists available at ScienceDirect

Global Ecology and Conservation

journal homepage: www.elsevier.com/locate/gecco

Phylogeography of two widespread C_4 grass species suggest that tableland and valley grassy biome in southwestern China pre-date human modification

Yingying Chu [a,b], Alison K.S. Wee [c,d,*], R. Sedricke Lapuz [a,b], Kyle W. Tomlinson [a,e,**]

[a] Center for Integrative Conservation, Xishuangbanna Tropical Botanical Garden, Chinese Academy of Sciences, Menglun, Yunnan 666303, China
[b] University of Chinese Academy of Sciences, No. 19A Yuquan Road, Beijing 10049, China
[c] Guangxi Key Laboratory of Forest Ecology and Conservation, College of Forestry, Guangxi University, Nanning, Guangxi, China
[d] School of Environmental and Geographical Sciences, University of Nottingham Malaysia, Semenyih 43500, Malaysia
[e] Center of Conservation Biology, Core Botanical Gardens, Chinese Academy of Sciences, Menglun, Yunnan 666303, China

ARTICLE INFO

Keywords:
Andropogoneae
Chloroplast DNA
Heteropogon contortus
Savanna
Themeda triandra
Yunnan-Guizhou Plateau

ABSTRACT

The Yunnan-Guizhou Plateau in southwest China lies at the intersection between East and South Asia, and is characterised by highly complex vegetation ranging from subtropical forest to open grassland. There is a long history of human modification to the landscape, but we know surprisingly little of the biogeography of open habitats such as grassy biomes in the region. To investigate the historical continuity of grassy biomes in southwest China, we examined the biogeographies and evolutionary histories of two widespread and dominant C_4 grasses, *Themeda triandra* and *Heteropogon contortus*, in Yunnan and southern Sichuan provinces, using chloroplast DNA markers in combination with climate data. We discovered that cool- and warm-adapted lineages have been widely distributed across the Yunnan-Guizhou Plateau for at least the last 2 million years, pre-dating any possible anthropogenic impact. Moreover, the high genetic diversity and strong spatial structure of both species suggests the continuous presence of multiple large populations, rather than a recent expansion from the dry valleys in response to anthropogenic deforestation. This is the first evidence for the long-term existence of extensive populations of C_4 grasses in this region outside the dry valleys, and calls for a reappraisal of the conservation value of these grass-dominated landscapes.

1. Introduction

Southwest China is dominated by the Yunnan-Guizhou Plateau (here after YGP), an area with tablelands > 1000 m and deeply incised valleys (Fig. 1), that formed as part of the complex folding in response to the collision between the Indian subcontinent and Asia (Metcalfe, 2017). The YGP lies at the intersection between the East and South Asian Monsoons (Shi and Chen, 2018; Shi et al., 2017). As a result, the YGP has a highly variable climate and edaphic space (Fig. 1) and complex vegetation ranging from dense tropical and subtropical forests in the south and west to open C_4 grasslands and savannas dominated by *Pinus yunnanensis* and *Quercus* spp.

* Corresponding author at: School of Environmental and Geographical Sciences, University of Nottingham Malaysia, Semenyih 43500, Malaysia.
** Corresponding author at: Center for Integrative Conservation, Xishuangbanna Tropical Botanical Garden, Chinese Academy of Sciences, Menglun, Yunnan 666303, China.
E-mail addresses: kimshan.wee@nottingham.edu.my (A.K.S. Wee), kyle.tomlinson@xtbg.org.cn (K.W. Tomlinson).

https://doi.org/10.1016/j.gecco.2021.e01835
Received 30 July 2021; Received in revised form 12 September 2021; Accepted 17 September 2021
Available online 20 September 2021

(hereafter referred to as 'grassy biomes') (Bond et al., 2019), in the north and east (Su et al., 2020).

In the YGP, as in much of monsoonal Asia, there is a long-standing perception that much of the vegetation which presently resembles savanna is degraded forest caused by human use of fire (Ratnam et al., 2011), but a growing body of evidence suggests that these communities may be better viewed as savannas as they are dominated by a distinct species-rich plant community adapted to open conditions and fire (Ratnam et al., 2016; Stott, 1988). Resolving whether the vegetation is forest or savanna has serious implications for how it should be managed; savannas depend on fire for their maintenance whereas forests are damaged by it (Ratnam et al., 2011). Presently, many countries in Asia, including China, have active fire suppression policies. The difficulty in resolving this debate is that humans have been manipulating fire for millenia in Asia. This behaviour is thought to have impacted natural vegetation (Gowlett, 2016), as persistent fire use increases the abundance of fire-adapted C_4 grassy biomes in tropical and sub-tropical regions (Bond et al., 2005). Therefore, one way to support vegetation being authentically savanna requires demonstrating that the vegetation has been

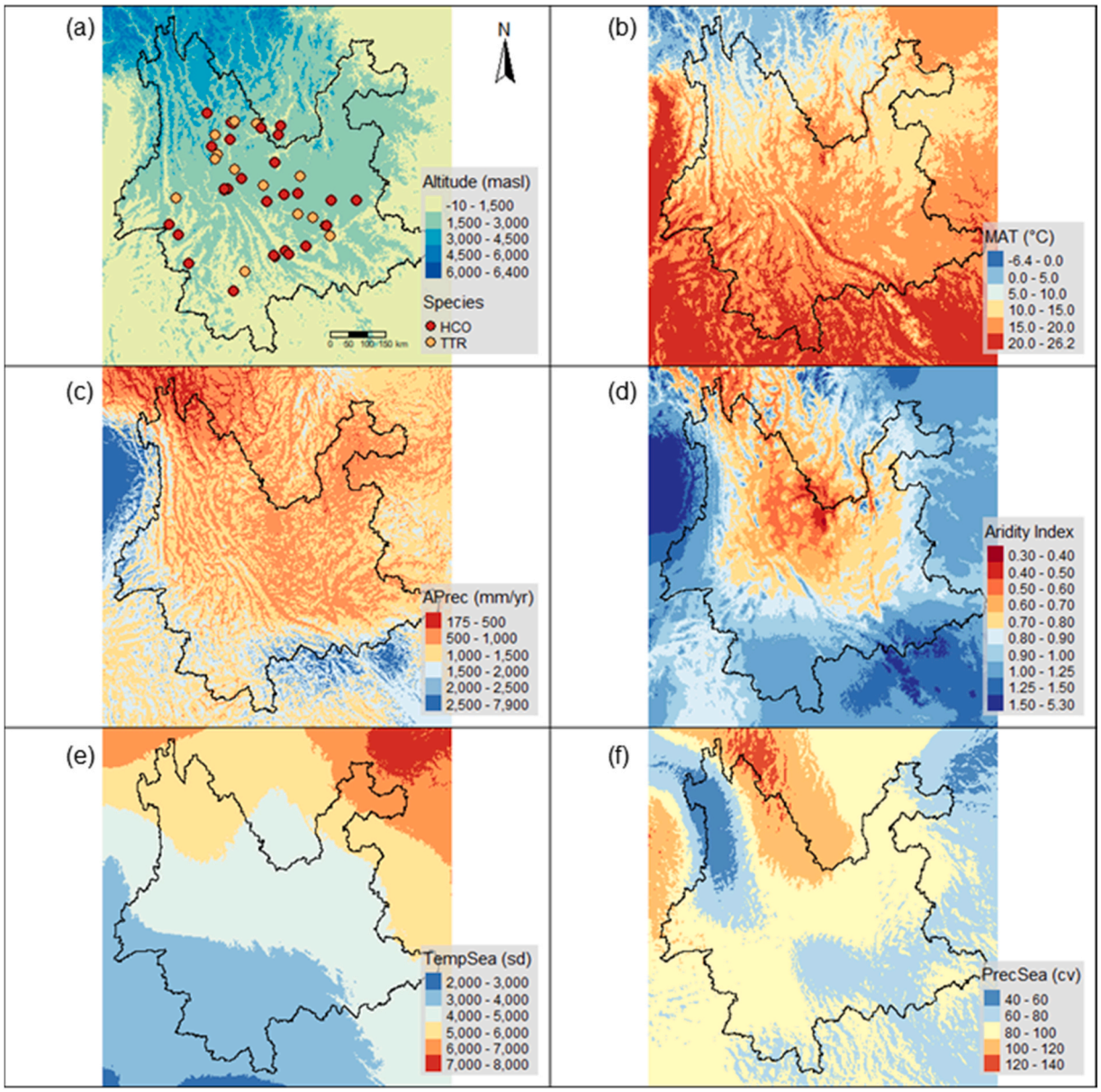

Fig. 1. Elevation and climate data for Yunnan-Guizhou Plateau (YGP), with the outline of Yunnan Province indicated. (a) Altitude (metres above sea level (masl)) with species locality for *Heteropogon contortus* (HCO) and *Themeda triandra* (TTR), (b) mean annual temperature (MAT; °C), (c) annual precipitation (AP, mm/year), (d) aridity index, (e) temperature seasonality (standard deviation), and (f) precipitation seasonality (coefficient of variation). The tablelands are shown in light blues and the valleys in yellows in panel (a). The data shows that the YGP has very strong environmental gradients, and the valleys can be detected by higher temperature and lower rainfall. There is also a strong north-south gradient in rainfall and aridity. (For interpretation of the references to colour in this figure legend, the reader is referred to the web version of this article.)

continuously present since before either the earliest evidence of hominins (strongest) or the earliest evidence of fire-use by humans (less strong). The earliest evidence for hominins in the YGP is ~ 1.7 Ma (Qian et al., 1991), and the earliest for Asia is ~2.1 Ma (Zhu et al., 2018). Early humans are thought to have started directly manipulating fire before~1.5 Ma in Africa (Gowlett, 2016), with the earliest evidence for fire-manipulation in East Asia at ~0.77 Ma (Shen et al., 2009). Thus, the minimum age of savanna fire-adapted vegetation in the region should be at least early Pleistocene to be considered authentic.

Until recently most vegetation of the YGP was classified as forest (Vegetation map of China 2000) (Su et al., 2020), with the exception of the deep valleys, which have much drier and more open grassy vegetation that was already recognised as savanna (Jin and Ou, 2000). The antiquity of the valley savannas is supported by fossil evidence from Yuanmou Valley indicating substantial C_4 presence and a switch from forest to grassy biomes at about 3.4 – 2 Ma (Biasatti et al., 2012; Yao et al., 2012), and molecular dating of a valley savanna endemic tree species, *Terminalia franchetii*, provides evidence that it has been present in the YGP for at least the last 1.4 – 4.2 Ma (Zhang et al., 2011). These data place the evolution of valley savannas prior to hominin presence or use of fire. So what remains unresolved is whether the *Pinus* and *Quercus*-dominated savannas of the vast tablelands of the YGP existed before human impacts on the landscape. There is palaeological evidence that *Quercus*-dominated landscapes have been present in the YGP since at least the late Miocene and that the dry climate present in Yunnan was established by the late Pliocene as evidenced by the extensive presence of sclerophyllous flora in northwest Yunnan that persists until today (Huang et al., 2016). Several other elements of the fossil flora suggest open landscapes were possible, including high richness of Rosaceae, Fabaceae and Rhamnaceae, but there are very few grass macrofossils recorded, although there is evidence for Poaceae pollen at several sites during the Pliocene-Pleistocene (Wu et al., 2019). Cumulative evidence from palaeological studies suggest the Pliocene-early Pleistocene may be the key period when the modern flora of Yunnan was established (Huang et al., 2016; Wu et al., 2019).

Due to the lack of grass fossils from the tablelands for the late Pliocene to early Pleistocene to date the age of grassy vegetation on the tablelands, we use phylogenetic evidence from savanna-adapted plant species to estimate the minimum age of savanna presence in the tablelands of the YGP. As it is already clear that savannas have existed in the valley areas since the late Pliocene/ early Pleistocene, we sought to determine whether the tested species possess distinct subclades adapted to valley or tableland climates that separated prior to hominin arrival or first use of fire by humans, and whether these clades have been present as established populations up to the present. There is good evidence that agrarian societies expanded in the YGP after the mid-Holocene climate optimum (Li et al., 2016; Ma et al., 2018; Zhang et al., 2014), and increased intensification of fire use may have resulted in a rapid expansion of grassy vegetation that led to its wide distribution observed today (Su et al., 2020). Hence the need for strong evidence of spatial population stability in the tested species from at least the early Pleistocene.

Grasses from the pantropical C_4 tribe Andropogoneae provide models to understand the history of grassy biomes in the YGP. They are shade-intolerant (Charles-Dominique et al., 2018), require open vegetation types to persist and dominate the understorey of fire-prone tropical savannas (Ripley et al., 2015). Recent phylogenomic evidence showed that Andropogoneae likely originated in East Asia in the Miocene, and later spread to Africa, Australia and the New World, through multiple independent dispersal events (Welker et al., 2020). Therefore, it is possible that the historical grassy biomes in the YGP and its surrounding regions supported the diversification of Andropogoneae. Due to their distribution across large gradients of temperature and rainfall, Andropogoneae grasses are known to form ecotypes that can be morphologically and ecologically distinctive (Beierkuhnlein et al., 2011; Downing and Groves, 1985; Malyshev et al., 2014). In the YGP, the climates of the valleys are hotter and drier than the adjacent tablelands (Fig. 1), so the conditions favour ecological divergence. Population differentiation of the species across the tablelands and valleys of the YGP could provide strong evidence that grassy ecosystems have existed there prior to hominin impacts.

Two perennial C_4 Andropogoneae grass species, *Themeda triandra* and *Heteropogon contortus*, are found extensively on both the tablelands and valleys across the YGP. These are two of the most widespread C_4 plants on earth, and are commonly found as herbaceous layer dominants in grasslands and savannas in Africa, Asia and Australia (Reynolds and Cumming, 2016; Rudov et al., 2020; Sage, 2017; Snyman et al., 2013) (electronic Supplementary Material, Fig. S1). A dated phylogeny focussed on *T. triandra* and *H. contortus* using globally collected samples agreed with the findings for Andropogoneae, that the major lineages of both species diversified in the Pleistocene and likely had an Asian origin (Arthan et al., 2021). However, comprehensive sampling in the region remains limited, usually with countries represented by only one or two samples. More detailed phylogeographies of these two species in Asia, especially East Asia, would elucidate on the lineage divergence and how environmental conditions in grassy biomes may have shaped genetic variation.

In this study we used chloroplast DNA-derived molecular data to examine the phylogeography of *T. triandra* and *H. contortus* across the tableland and valley grasslands in the YGP. We tested the hypotheses that (1) there are extant populations of both species in the valley and tableland systems in the YGP that predate the earliest known presence of humans, (2) the prolonged existence of tableland and valley populations gave rise to lineages adapted to distinct climate conditions, and (3) grassland communities persisted without contraction through the Holocene, and without rapid colonisation from refugia. Based on these hypotheses, we predicted that in both species: (1) the divergence time of major genetic lineages in each species is dated to more than 2.1 Mya, (2) haplotype composition differs significantly between climates associated with the valley and tableland systems in the YGP, (3) the level of genetic diversity is similar between the valley and tableland populations and shows no signs of historical contraction. These predictions, if all met, would provide supportive information that C_4 grassy biomes have been extensively distributed across the YGP throughout the Pleistocene and Holocene, independently of human impacts.

2. Materials and methods

2.1. Sample collection

A total of 187 individuals from 21 populations for *T. triandra* and 319 individuals from 34 populations for *H. contortus* were sampled across Yunnan province and southern Sichuan Province (Table 1, see associated locational and climate data in electronic Supplementary Material Table S6). Taking into account the influence of asexual reproduction of grasses, fresh leaf tissue was sampled off

Table 1
Details of locations, sample size (N), number of haplotypes (n), haplotype diversity (h) and nucleotide diversity (π) of 21 *T. triandra* populations (top) and 34 *H. contortus* populations (bottom).

Location	Code			cpDNA		
		Altitude (m)	N	No. of haplotypes (n)	h	π
Themeda triandra						
Binchuan	BC	2500	9	3	0.417	0.00053
Chenghai	CH02	1891	10	1	0	0
Chengjiang	CJ	1856	10	1	0	0
Chuxiong	CX	1863	9	1	0	0
Dali	DL	2436	9	4	0.694	0.00149
Fumin	FM	1702	10	4	0.694	0.00112
Huaping	HP	1642	8	3	0.464	0.00059
Lancang	LC	1640	9	2	0.500	0.00043
Lijiang	LJ	2052	6	1	0	0
Longtan	LT	936	9	4	0.694	0.00154
Ninger	NE	1470	9	1	0	0
Pengpu	PP	1520	10	4	0.800	0.00104
Panxi	PX	1399	9	3	0.667	0.00082
Shidian	SD	1734	10	2	0.200	0.00052
Shilin	SL	1704	9	2	0.222	0.00039
Shiping	SP	1679	7	3	0.524	0.00091
Shizong	SZ	1932	6	2	0.533	0.00139
Wase	WS	2425	9	2	0.389	0.00034
Xiangyun	XY	2095	9	2	0.500	0.00130
Yongsheng	YS	2271	10	2	0.200	0.00017
Yuxi	YX	2089	10	3	0.511	0.00089
Heteropogon contortus						
Anding	AD	1660	4	3	0.833	0.00993
Anning	AN	2349	10	4	0.778	0.00187
Chenghai	CH01	2670	10	3	0.378	0.00102
Chenghai	CH02	1891	10	3	0.600	0.00232
Chengjiang	CJ	1856	10	2	0.356	0.00040
Chuxiong	CX01	1957	10	2	0.467	0.00105
Dali	DL	2436	9	2	0.222	0.00200
Fumin	FM	1702	9	2	0.389	0.00087
Huaping	HP	1642	10	3	0.644	0.00142
Lancang	LC	1640	8	2	0.571	0.00128
Lufeng	LF	1413	10	2	0.467	0.00105
Lijiang	LJ01	2165	9	2	0.222	0.00025
Longtan	LT	936	10	1	0	0
Mojiang	MJ	1850	4	3	0.833	0.00581
Nanjian	NJ01	1483	10	5	0.822	0.00185
Nanjian	NJ03	1515	11	3	0.636	0.00143
Nanjian	NJ04	1987	10	2	0.467	0.00105
Puer	PE	1231	10	3	0.644	0.00147
Pengpu	PP	1520	10	3	0.511	0.00192
Panxi	PX02	1644	9	2	0.222	0.00150
Qina	QN	1358	10	3	0.644	0.00107
Renhe, Sichuan	RH	1563	10	3	0.644	0.00142
Rongjiang	RJ	1190	9	1	0	0
Shidian	SD	1734	10	2	0.533	0.00120
Shilin	SL	1704	10	3	0.600	0.00097
Shiping	SP	1679	9	1	0	0
Shizong	SZ	1932	9	2	0.222	0.00075
Tianshentang	TS	2189	10	2	0.467	0.00105
Xiangyun	XY	2095	10	2	0.467	0.00105
Yanbian, Sichuan	YB	1510	10	2	0.200	0.00045
Yuanjiang Station	YJS	645	9	2	0.389	0.00350
Yuanmou	YM	1411	10	2	0.200	0.00045
Yimen	YME	1509	10	4	0.644	0.00232
Zhenkang	ZK	696	10	1	0	0

grass plants at least 5 m apart. Leaf samples were preserved in silica gel. Total genomic DNA was extracted using a Plant Genomic DNA Extraction Kit (Cat: DP350, Tiangen, Beijing, China) according to manufacturer's protocols.

2.2. Chloroplast DNA analysis

Chloroplast DNA (cpDNA) analysis was done using primers developed in this study. Whole chloroplast genomes of *T. triandra* (accession numbers KY707767, KY707770, KY707771 and KY707772) and *H. contortus* (accession numbers NC035027 and KY596145) were downloaded from NCBI Genbank and aligned. Variable regions were identified, and primer sequences were designed using Primer3 (Untergasser et al., 2012; Koressaar and Remm, 2007). A total of nine primer pairs were tested, but only two primer pairs per species produced consistent amplification and polymorphic cpDNA fragments across our samples.

Based on our marker development results, each species was genotyped with one shared cpDNA region (psbI-psbD intergenic spacer, IGS) and another region that was different between the species (ndhF-rpl32 IGS region for *T. triandra* and rpoC2 region for *H. contortus*). Primer sequences for psbI-psbD, ndhF-rpl32 and rpoC2 were listed in Table S7. The PCR was performed in a 50 μL reaction mixture containing 1.0 μL genomic DNA, 5.0 μL of 10× PCR buffer,2.0 μL of 10 Mm dNTPs, 1.0 μL of 5 pM of each primer and 0.3 μL of Taq polymerase. The amplification protocols were 5 min denaturation at 95 ℃, then 30 cycles of 1 min denaturation at 95 ℃, 1 min annealing at 55 ℃, and 1 min extension at 72 min; with a final 7 min extension at 72 ℃. All of the high-quality PCR products were sequenced using the amplified forward and reverse primers with an ABI3700 Sequence Analyzer platform (Applied Biosystems). Different regions were employed in the two species to ensure consistent amplification and substantial variation in the amplified fragments. The total genotyped sequences were 1154 bp and 890 bp for *T. triandra* and *H. contortus*, respectively. Subsequent analyses were conducted independently for each species.

2.3. Genetic diversity

Parallel chromatograms derived from the ABI3700 platform were contrasted for accuracy by visual inspection using SeqTrace-0.9.0 (Stucky, 2012). DNA sequences were aligned by clustalW aligner algorithm and combined in Mega v7.0.26 (Kumar et al., 2016) with minor subsequent adjustments. The ragged tails of the alignments were trimmed to ensure a uniform ending. All sequences were assigned to different haplotypes using GenAlEx v6.51 (Peakall and Smouse, 2012). Genetic diversity indices, including the number of haplotypes (n), haplotype diversity (h) and nucleotide diversity (π) were estimated for each population using DnaSP5 v5.0 (Librado and Rozas, 2009). The neutrality indices (Tajima's D and Fu's Fs) and total genetic differentiation (F_{ST}) were estimated using DnaSP5 v5.0 (Librado and Rozas, 2009). A two-samples t-test was conducted using Origin (Origin2019, 2019) to compare the n, h and π, between the tableland and valley populations in each species. The tableland and valley populations were defined in the subsequent section on "*Relationship between genetic structure and environmental gradients*". In brief, these populations were defined by distinct lineages found in the phylogenetic analysis that differed with respect to mean annual temperature (cool-adapted versus warm-adapted lineages).

2.4. Phylogeographic analysis

For each species, a haplotype distribution map was generated through GeneGIS (Parks et al., 2009). In addition, an unrooted parsimony haplotype network was constructed using the TCS method implemented in POPART v1.7 (Leigh and Bryant, 2015).

The phylogenetic tree for each species was constructed using all haplotypes found in Yunnan, *Paspalum paniculatum* as an outgroup, 11 other species from Andropogoneae to balance the tree, and 10 – 11 conspecific samples taken from outside the YGP to allow for better comparison with recent studies on the global evolutionary history of *Themeda* and *Heteropogon* (Arthan et al., 2021; Welker et al., 2020). The chloroplast genomes of the additional taxa were downloaded from NCBI Genbank (see electronic Supplementary Material, Table S8) and the sequences of the cpDNA regions used in this study was extracted from them.

The phylogenetic tree was constructed by means of maximum parsimony (MP) and maximum likelihood (ML) using MEGA v7.0.26 (Kumar et al., 2016), and Bayesian inference (BI) using MrBayes (Ronquist et al., 2012). For the ML and BI analysis, the best-fit nucleotide substitution model was determined using jMODELTEST v2.1.4 (Darriba et al., 2012) with default options and applying the Bayesian Information Criterion (BIC). The HKY and GTR mutation models were selected for *T. triandra* and *H. contortus* respectively. The ML and MP analyses were both conducted with 5000 bootstrap replicates. The BI analysis was conducted using Markov Chain Monte Carlo (MCMC) chains that ran for 2,000,000 generations. To ensure the efficiency of the MCMC method, standard deviation of split frequencies was confirmed to be below 0.01 and potential scale reduction factor (PSRF) was reasonably close to 1.0 for all parameters after MCMC runs.

2.5. Divergence time estimation

The divergence time of major lineages was estimated for both species using BEAST 2.5.2 (Drummond and Rambaut, 2007). For consistency, the same dataset and nucleotide substitution models as the phylogenetic tree reconstruction were used. The site model was implemented with four gamma rate categories. A relaxed lognormal clock model was applied. Due to limited fossil record for our study species, we adopted a secondary calibration approach based on the divergence of Arundinelleae+Andropogoneae with a mean of 19.1 Ma, a normal distribution and a standard deviation of 0.155 (Vicentini et al., 2008). To assess the impact of priors on the molecular dating, we tested an alternative and commonly used secondary calibration point at the divergence between *Zea mays* and the

rest of Andropogoneae at 15.26 Ma with a normal distribution and a standard deviation of 0.0001 (Christin et al., 2014). These two priors were used as calibration points in most recent studies of Andropogoneae (Arthan et al., 2021; Dunning et al., 2017; Welker et al., 2020), thus allowing for easier comparison with other published data. Four independent Markov Chain Monte Carlo (MCMC) analyses were run for 200,000,000 generations, with 10% of the trees discarded as burn-in. Convergence and ESS were verified in Tracer v.1.5 (Drummond and Rambaut, 2007). The maximum clade credibility trees were obtained from all runs and the final chronograms were drawn using FigTree v.1.4.4 (Drummond and Rambaut, 2007).

2.6. Relationship between genetic structure and environmental gradients

To address our third hypothesis, that the two grass species possess lineages representing cooler-adapted lineages found on the tablelands and hotter-adapted lineages found in the valleys, we tested whether the mean values of five climate variables could be distinguished with respect to the major haplotype clusters identified via the haplotype network and phylogeny analyses: Mean annual temperature (MAT) and Annual precipitation (AP) have been shown to differ among populations or ecotypes of grass species (Beierkuhnlein et al., 2011; Downing and Groves, 1985; Malyshev et al., 2014), with MAT useful to define hot valley versus cool tableland differences; Aridity index is a measure of the water stress that plants are subjected to, and is defined as the ratio of AP over potential evapotranspiration (Trabucco and Zomer, 2018); Precipitation seasonality is considered to be a significant correlate of the distribution of grassy biomes (Lehmann et al., 2014), and temperature seasonality is likely differentiated in the YGP between higher-elevation tablelands that are exposed to climate fluctuations and less-exposed valley locations. Data for MAT, AP, temperature seasonality and precipitation seasonality for each population were extracted from CHELSA v1.2 at 30″ (Karger et al., 2017a, 2017b) grid resolution. Aridity index was taken from Trabucco and Zomer (2018) at 30″ grid resolution. We used the lm() function in R v4.0.0 (R Core Team, 2020) with haplotype clusters as factor predictors and climate variables as response variables, with separate runs for each environmental variable and each species. Significant differences between clusters were first tested with ANOVA type II, and when significant, were followed by Tukey HSD adjusted pairwise tests.

2.7. AMOVA analysis

AMOVA (Analysis of Molecular Variance) allows the hierarchical partitioning of genetic variation among populations and groups. We used the Φ-statistic to estimate population genetic differentiation for haploid data. We processed four independent AMOVA analyses through GeneAlEx 6.5 (Peakall and Smouse, 2012) with 999 permutations to determine the partitioning of genetic variation under three scenarios: (1) populations were grouped according to the most significant climate variable in the ANOVA type II test above; (2) populations were grouped according to paleo-drainage systems of the YGP (Zhang et al., 2011) to test the effects of the river capture events; (3) populations were grouped according to current river pattern of the YGP (Wu, 2004) (populations included in each group are provided in Table S9, electronic Supplementary Material). Based on the outcome of the regression tests above, MAT (Mean annual temperature) was chosen as the environment variable to test the partitioning of genetic variation, with 15.5 °C and 17.5 °C were used as the cut-offs to divide populations into two groups for *T. triandra* and *H. contortus*, respectively.

Table 2
Neutrality tests (Tajima's D, Fu's Fs) and *t*-tests of no. of haplotypes, haplotype diversity and nucleotide diversity between tableland and valley populations for *Themeda triandra* and *Heteropogon contortus*.

		Test statistics	p-value	df	Genetic parameter means
Neutrality test					
Tajima's D	*T. triandra*	0.524	> 0.10		
	H. contortus	-0.999	> 0.10		
Fu's Fs	*T. triandra*	0.118	0.999		
	H. contortus	-2.491	0.997		
t-test (tableland vs valley)					
No. of haplotypes (n)					
	T. triandra	-0.594	0.560	18.732	2.22 (tableland) 2.50 (valley)
	H. contortus	0.420	0.679	19.923	2.47 (tableland) 2.33 (valley)
Haplotype diversity (*h*)					
	T. triandra	-0.276	0.785	18.774	0.36 (tableland) 0.39 (valley)
	H. contortus	1.058	0.301	23.291	0.48 (tableland) 0.39 (valley)
Nucleotide diversity (π)					
	T. triandra	0.276	0.793	15.191	0.000678 (tableland) 0.000613 (valley)
	H. contortus	1.432	0.164	25.868	0.00192 (tableland) 0.00109 (valley)

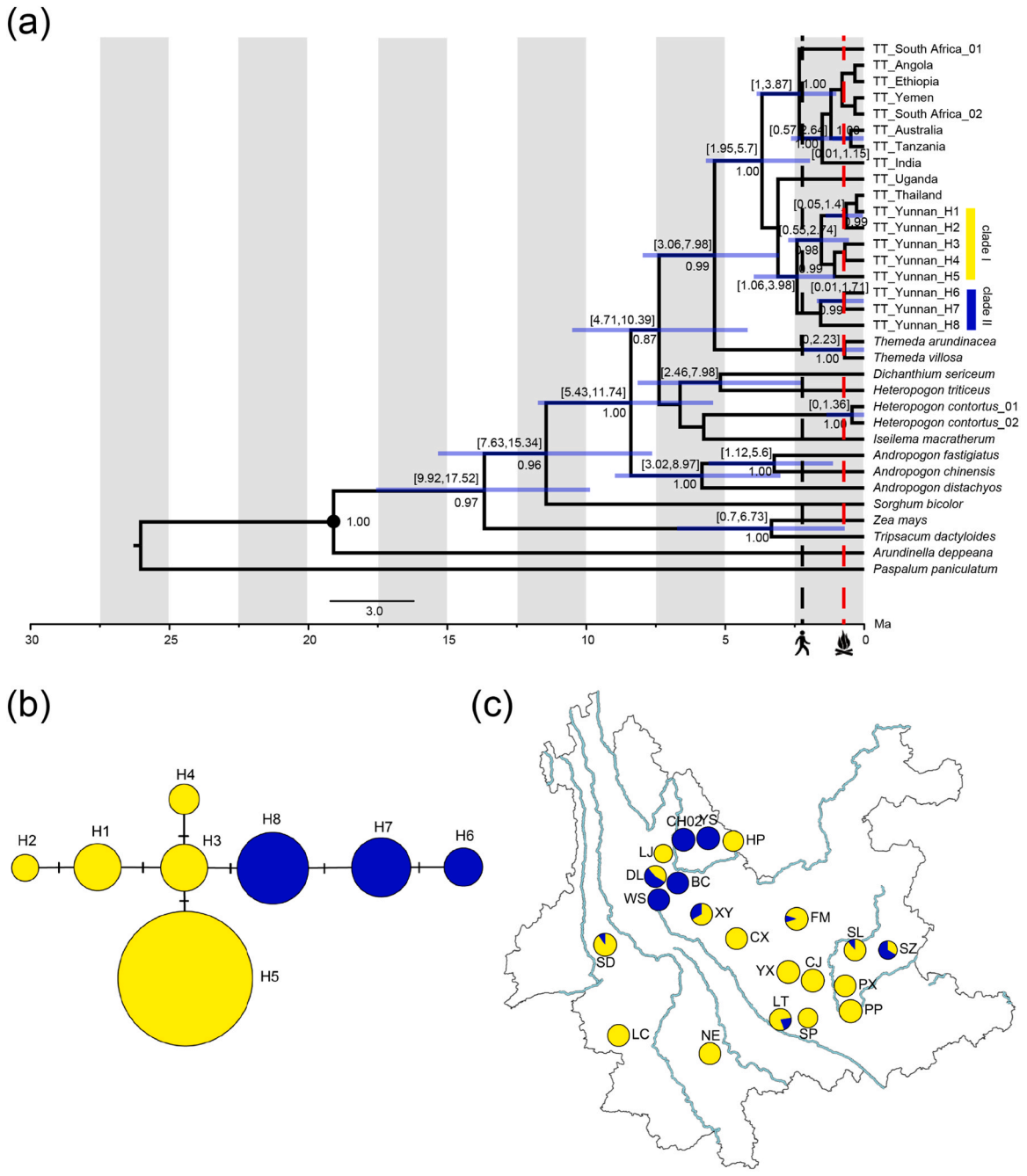

Fig. 2. Phylogeography analyses and divergence time estimation for *Themeda triandra,* showing (a) the phylogenetic tree generated from the divergence time estimation by BEAST, (b) the haplotype network, (c) the geographical distribution of cpDNA haplotypes by clade and populations, and haplotypes in (b) and (c) are coloured based on the clades in the phylogenetic tree. Clade I (the blue lineage) is the cooler-adapted tableland lineage and Clade II (the yellow lineage) is a warmer-adapted valley lineage (see Fig. 4). Circle size in (b) and (c) represents the number of individuals. The number of perpendicular lines on the branches in (b) indicate the mutational steps between haplotypes. In (a), the blue bars and bracketed values represent the 95% HPD of the divergence times. The numbers beside the node indicate the node support from divergence time estimation tree. Only support values above 0.8 are shown. The red vertical dash line on the x-axis denotes the time point when humans started using fire in Asia. The black vertical dash line on the x-axis denotes the time point when hominins were present in Asia. The black circle denotes the calibration point. (For interpretation of the references to colour in this figure legend, the reader is referred to the web version of this article.)

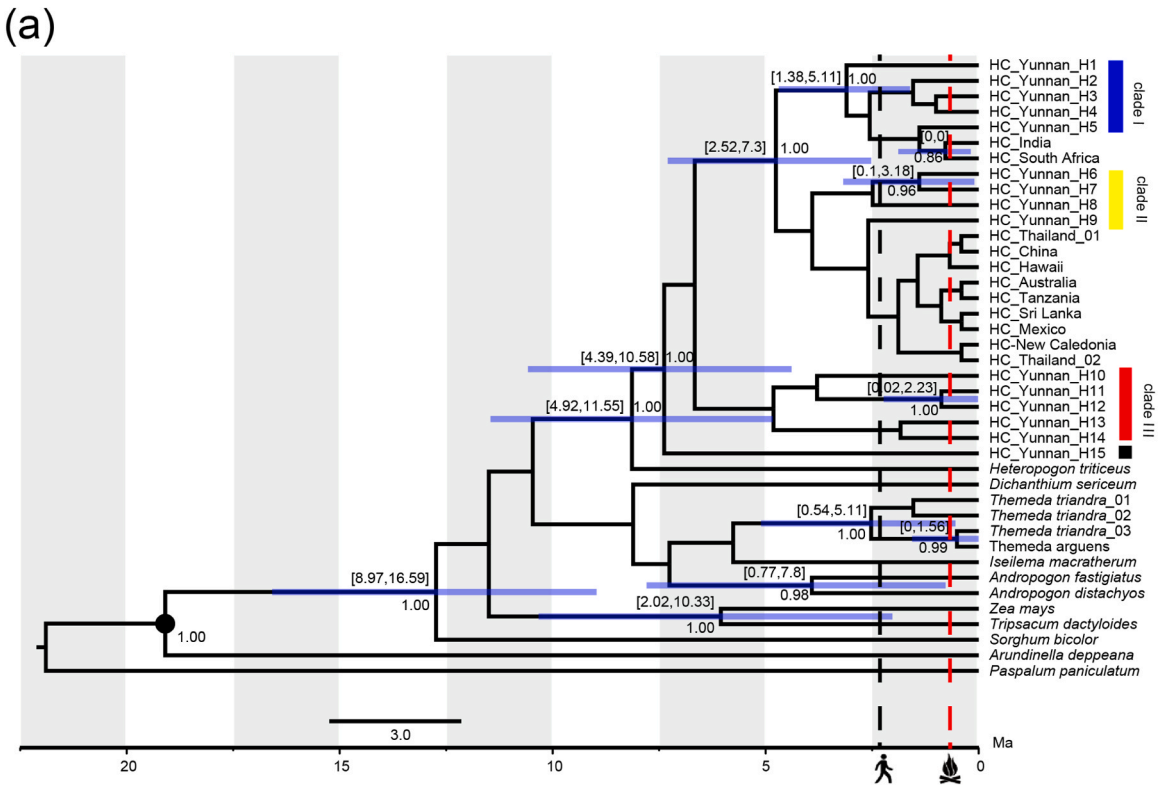

(caption on next page)

Fig. 3. Phylogeography analyses and divergence time estimation for *Heteropogon contortus,* showing (a) the phylogenetic tree generated from the divergence time estimation by BEAST, (b) the haplotype network, (c) the geographical distribution of cpDNA haplotypes by clade and populations, and haplotypes in (b) and (c) are coloured based on the clades in the phylogenetic tree. Clade I (the blue lineage) is the cooler-adapted tableland lineage, Clade II (the yellow lineage) is a warmer-adapted valley lineage, and Clade III is an older lineage found in intermediate temperatures (see Fig. 4). Circle size in (b) and (c) represents the number of individuals. The number of perpendicular lines on the branches in (b) indicate the mutational steps between haplotypes. In (a), the blue bars and bracketed values represent the 95% HPD of the divergence times. The numbers beside the node indicate the node support from divergence time estimation tree. Only support values above 0.8 are shown. The red vertical dash line on the x-axis denotes the time point when humans started using fire in Asia. The black vertical dash line on the x-axis denotes the time point when hominins were present in Asia. The black circle denotes the calibration point. (For interpretation of the references to colour in this figure legend, the reader is referred to the web version of this article.).

3. Results

3.1. Genetic diversity

At the species level, both *T. triandra* ($h = 0.679$) and *H. contortus* ($h = 0.638$) had comparable levels of haplotype diversity. However, the number of haplotypes (n) and nucleotide diversity (π) in *H. contortus* (n = 15; $\pi = 0.00216$) doubled that of *T. triandra* (n = 8; $\pi = 0.00130$). Therefore, *T. triandra* had lower genetic diversity than *H. contortus*.

The number of haplotypes per population ranges between 1 and 5 in both species, with an average of 2.4. In *T. triandra*, the highest genetic diversity was found in the LT population, whereas the LT *H. contortus* population was fixed for a single haplotype (Table 1). Instead, the highest haplotype and nucleotide diversity in that species was detected in the AD population (Table 1). Fixation of haplotype (i.e., the presence of only one haplotype) was found in 24% and 12% of populations in *T. triandra* (CH02, CJ, CX, LJ, NE) and *H. contortus* (LT, RJ, SP, ZK), respectively.

The total population differentiation (F_{ST}) was also comparable between the two species: 0.518 for *T. triandra* and 0.453 for *H. contortus.* Neutrality tests of Tajima's D and Fu's Fs showed positive and non-significant negative values in Table 2, suggesting neutral selection and demographic equilibrium in both species. A *t*-test comparison revealed no significant difference in the number of haplotype (n), haplotype diversity (h) and gene diversity (π) between tableland and valley populations of both species (Table 2).

3.2. Phylogeography

In *T. triandra*, the cpDNA haplotypes from the YGP formed a monophyletic clade consisting of two major, well-supported lineages (Fig. 2a; Fig. S3). Clade I consisted of three haplotypes that were mostly distributed at higher elevations in northwestern and eastern Yunnan (Fig. 2a, c). Clade II consisted of the remaining five haplotypes, including the dominant H5 that was found in 52.94% of sampled individuals (Fig. 2a, c). The topology of the haplotype network concurred with that of the phylogenetic tree, showing that the haplotypes formed two major clusters (Fig. 2b). All haplotypes were separated by only one mutational step, indicating recent divergence among these haplotypes. The monophyletic clade of YGP samples were nested inside the phylogenetic clade of *T. triandra* that included external (non YGP) samples (Fig. 2a) suggesting immigration of *T. triandra* into Yunnan.

In contrast, the phylogenetic relationship among *H. contortus* haplotypes from Yunnan revealed a more complex genetic pattern. The phylogenetic tree consisted of three major clades (Fig. 3a; Fig. S4). Clade I and Clade II consisted of the two dominant haplotypes, H3 and H8, which was shared among 47.37% and 48.28% of *H. contortus* individuals from Yunnan, respectively. In comparison, Clade III was small, and only consisted of five haplotypes found in 3.45% of all Yunnan individuals. Haplotypes in Clade III were mainly distributed in three adjacent sites YJS, AD and MJ (Fig. 3c). Like *T. triandra,* the topology of the *H. contortus* haplotype network concurred with its phylogenetic tree. However, the haplotypes in *H. contortus* were separated by at most six mutational steps (Fig. 3b), indicating a deeper divergence between clades as compared to *T. triandra.* Moreover, the haplotype clades of *H. contortus* sampled in the YGP encompassed all samples collected outside the YGP, suggesting emigration of *H. contortus* out of the YGP.

3.3. Divergence time estimates

The dated phylogenies using each of the two fossil calibration points produced highly congruent outcomes in terms of topology and divergence time estimation. Here, we present the dated phylogeny calibrated with the divergence of Arundinelleae+Andropogoneae; the dated phylogeny with the other calibration point (*Zea mays*+Andropogoneae) is provided in Fig. S5.

Our results demonstrated that the two major *T. triandra* clades in Yunnan diverged before 1.06 Ma (95% Highest Posterior Density, HPD: 3.98–1.06 Ma) (Fig. 2a). In *H. contortus*, the two major clades in Yunnan, Clade I and Clade II (along with samples from beyond China), diverged before 2.52 Ma (95% HPD: 7.3–2.52 Ma). *H. contortus* and *H. triticeum* diverged at 7.49 Ma (95% HPD:10.58–4.39 Ma) (Fig. 3a).

3.4. Relationship between genetic structure and environmental gradients

The phylogeny identified two major haplotype clusters in *T. triandra* and three major clusters in *H. contortus* (Figs. 2 and 3). For *T. triandra*, the two haplotype clusters significantly differed with respect to mean MAT, aridity, temperature seasonality and precipitation seasonality of their location of occurrence, but not in AP (electronic Supplementary Material, Table S10). Specifically, Cluster II

was found in cooler, more arid (lower aridity index) environments that were also more seasonal with respect to temperature and precipitation than Cluster I (Fig. 4). For *H. contortus*, significant difference was detected among the clusters in terms of MAT, aridity, temperature seasonality and precipitation seasonality, but not AP (Table S10). The small cluster, Cluster III was associated with a less water-stressed environments (greater AP and lower precipitation seasonality) and the two larger clusters, I and II, were significantly different with respect to MAT alone. In both species, MAT had the highest explanatory power to explain climate differences between haplotype clusters. The division between the major clusters of *T. triandra* with respect to MAT was about 15.5 °C. The division between the major clusters of *H. contortus* with respect to MAT was about 17.5 °C.

3.5. AMOVA analysis

The AMOVA results indicated that in both species, no significant genetic variation was found among groups divided by paleo-river systems and current river systems. Both species showed significant genetic variation among groups ($P < 0.001$) when populations were divided by MAT, with *T. triandra* having a larger partition of genetic variation among these groups than *H. contortus* (Table 3).

4. Discussion

4.1. C_4 grassy biomes as natural ecosystems on the tablelands of Yunnan-Guizhou Plateau

This study used molecular evidence to challenge the notion that grassy biomes on the Yunnan-Guizhou Plateau (YGP), southwest China, are anthropogenically derived ecosystems. Chloroplast DNA data from two dominant C_4 grass species, *T. triandra* and

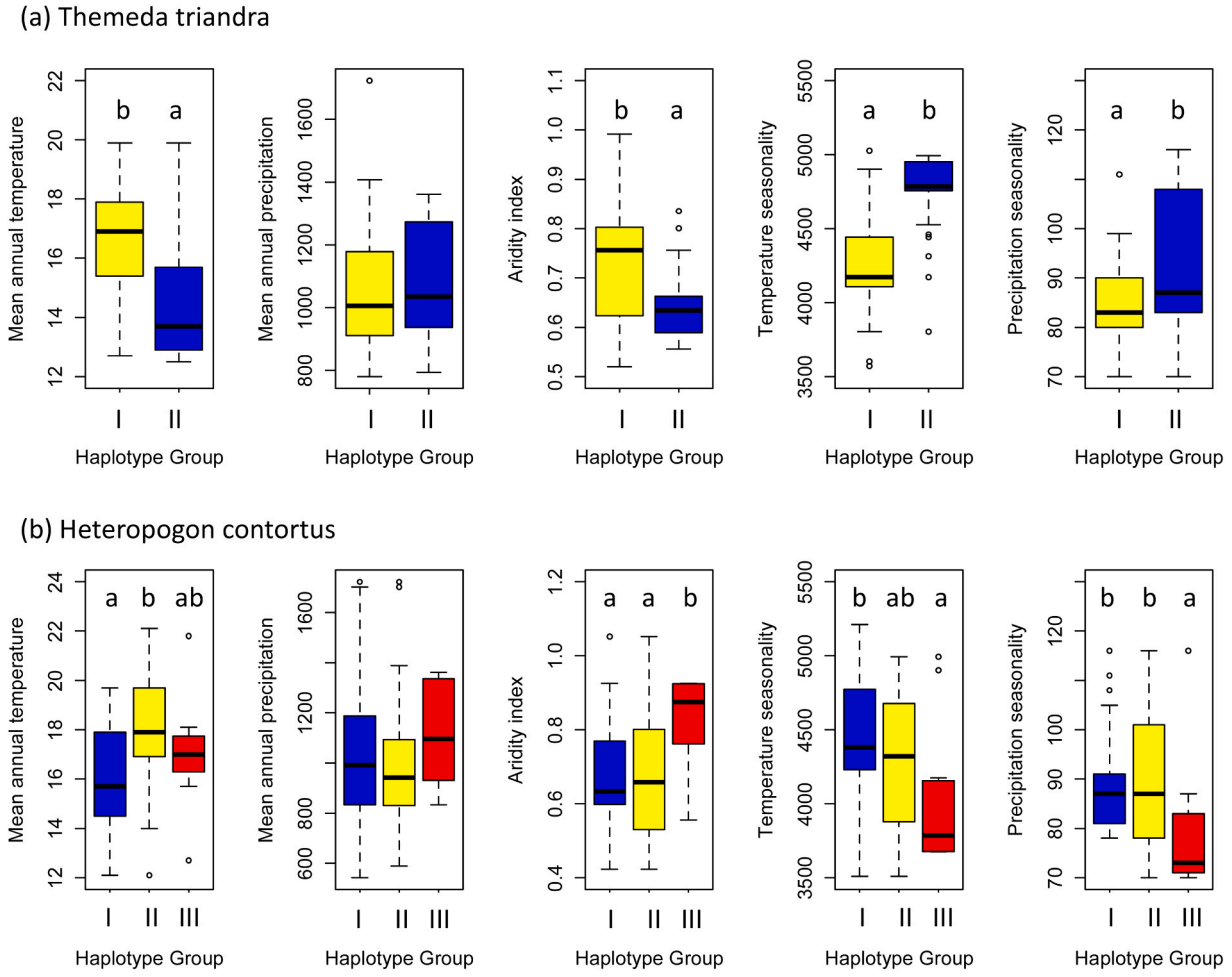

Fig. 4. Differences in mean climate parameters between haplotype clades in *Themeda triandra* (2 clades; Panel A) and *Heteropogon contortus* (3 clades; Panel B). Letters indicate non-significant differences between groups based on Tukey HSD pairwise tests conducted only when significant variation in climate parameters between groups were detected using ANOVA (electronic Supplementary Material, Table S10). Panels without letters indicate variables for which significant variation between groups was not detected. Colours and clade numbers are aligned with Figs. 2 and 3.

Table 3
AMOVA results comparing the genetic variation among groups.

	df	SS	MS	Percentage variation (%)	*Φ*-statistics
Themeda triandra					
Mean annual temperature (2 groups)					
Among groups	1	11.781	11.781	11	0.111***
Among populations	19	67.328	3.544	44	0.495***
Within populations	166	60.473	0.364	45	0.551***
Paleo river systems (7 groups)					
Among groups	6	24.957	4.159	2	0.018*
Among populations	14	54.152	3.868	51	0.519***
Within populations	166	60.473	0.364	47	0.527***
Current river systems (5 groups)					
Among groups	4	16.395	4.099	0	0.000
Among populations	16	62.715	3.920	53	0.525***
Within populations	166	60.473	0.364	47	0.526***
Heteropogon contortus					
Mean annual temperature (2 groups)					
Among groups	1	17.653	17.653	9	0.085***
Among populations	32	123.271	3.852	34	0.377***
Within populations	285	164.719	0.578	57	0.430***
Paleo river systems (7 groups)					
Among groups	6	19.804	3.301	0	-0.029
Among populations	27	121.119	4.486	42	0.418***
Within populations	285	164.719	0.578	58	0.401***
Current river systems (5 groups)					
Among groups	4	14.476	3.619	0	-0.015
Among populations	29	126.447	4.360	41	0.412***
Within populations	285	164.719	0.578	59	0.403***

df; degree of freedom. SS; sum of square. MS; mean of square.
* Significant at $P < 0.05$ level.
*** Significant at $P < 0.001$ level.

H. contortus, demonstrated that major lineages in both species were widely distributed across the YGP since at least the mid-Pleistocene. For *H. contortus*, the minimum date between the two major valley and tableland clades is 2.52 Ma (Fig. 3a), substantially earlier than 2.1 Ma, the earliest known date of hominins in east Asia (Zhu et al., 2018). For *T. triandra*, the minimum date of the divergence between the major valley and tableland clades is 1.06 Ma (Fig. 2a), which is later than the earliest evidence for hominins, but earlier than the earliest known use of fire by humans in Asia at 0.77 Ma (Shen et al., 2009). This provides novel evidence that the occurrence of grassy biomes in both the valleys and tablelands in the YGP pre-dates human modification of landscape fire regimes.

Furthermore, the genetic and haplotype diversity in both species were similar or higher than other Andropogoneae grasses previously surveyed in the region (Liu et al., 2018; Shang et al., 2019; Yan et al., 2015; Yang et al., 2018). Therefore, the congruent results in both dominant species provide unequivocal evidence of the deep divergence of major clades. AMOVA tests indicated that the phylogeographic pattern of *T. triandra* and *H. contortus* populations were better explained when grouped by the mean annual temperature (MAT) of the sites than by other spatial barriers previously shown to be of importance in the YGP (Jiang et al., 2017; Ju et al., 2018; Zhao and Gong, 2015). Importantly, haplotype Cluster II of *T. triandra* and Cluster I of *H. contortus* were associated with cooler climates of the YGP, indicating the long-term existence of the species on the tablelands of the YGP. To our knowledge, this data is complimentary to all existing evidence for C_4 grassy biomes in the YGP, which have only found evidence for pre-hominin C_4 species in the valleys (Biasatti et al., 2012; Yao et al., 2012). It should be noted that the age of grass evolution remains unresolved and importantly that combined phytolith and macrofossil data suggest that grasses may have evolved earlier than most present phylogenies assume (see Spriggs et al., 2014, Schubert et al., 2019). If this is shown to be true then our dates are underestimated, meaning that C_4 grassy biomes arrived even earlier in the YGP.

4.2. High genetic diversity and strong population subdivision

Our data provided four lines of evidence that both *T. triandra* and *H. contortus* have persisted as multiple large, subdivided populations in the YGP for generations: (i) high genetic diversity, (ii) strong genetic differentiation, (iii) no evidence of population expansion or contraction, and (iv) a similar level of genetic diversity between tableland and valley populations. Within each of our study species, similar levels of genetic diversity (in number of haplotypes, haplotype diversity and gene diversity) between tableland and valley populations further point towards both population groups having equally long evolutionary history in the YGP. In addition, population expansion or contraction was not detected in the neutrality tests, suggesting that the patterns of genetic diversity are not influenced by population demography. The long-term persistence of the cooler-tolerant haplotype clades of each species through the glaciations and interglaciations of the Pliocene and Tertiary, as well as their strong genetic differentiation, may have been supported by the geography and history of the YGP. First, the rugged and deeply incised terrain of the YGP (see Fig. 1), likely allowed the haplotype groups to track temperature variation through the glacial-interglacial cycles. Second, the YGP remained ice-free throughout the

glaciation periods with the southern ice-sheet over Tibet not extending below 3800 m in the Hengduan mountains to the northwest of the YGP (Kuhle, 2011) and similarly the permafrost maximum extent did not go further south than the Hengduan mountains (Vandenberghe et al., 2014).

Generally, population genetic structure is more prominent in species with restricted gene flow, habitat fragmentation and ecological disturbance. The genetic differentiation among populations in *T. triandra* and *H. contortus* indicates a high level of population subdivision, with F_{ST} values of 0.518 and 0.453 respectively. This concurs with genetic data from other species from the YGP, with F_{ST} values for the C_4 grass *Miscanthus sinensis* of 0.561 (Yan et al., 2015), and F_{ST} of 0.866 and 0.98 with $>$ 70% of genetic variation being partitioned among populations for two tree species, *Quercus aquifolioides* and *Terminalia franchetii* (Du et al., 2017; Zhang et al., 2011). Such strong, universal population subdivision across plant species could be attributed to the complex biogeographical history and or environmental heterogeneity of the region that increased insularity among populations.

4.3. Phylogeographic pattern dictated by climate not biogeographic history

The phylogeographic pattern in *T. triandra* and *H. contortus* in the YGP do not concur with that of woody plants in this region, suggesting fundamental differences in geographic constraints between the grasses and the trees. The trees that occupy drier sites in the YGP have a distinctive phylogeographic divide along the Tanaka line, which runs NW – SE along the tableland dividing the Yuanjiang valley from the Jinshajiang (Yangtze) valley (Jiang et al., 2017; Ju et al., 2018; Zhao and Gong, 2015). This divide was absent in our grass species; haplotypes that were associated with warmer temperatures were present in both Yuanjiang and Jinshajiang valleys.

Effects of isolation by environment (IBE) may be different for woody and herbaceous species across the complex landscape in southwestern China because of their different life-forms. Among the tree species, *Bombax ceiba* is restricted to hotter, frost-free climates in the valleys, and *Q. kerrii* is restricted to cooler, temperate climates on the tablelands. Therefore, cool tablelands and hot valleys could present strong dispersal barriers to *B. ceiba* and *Q. kerrii*, respectively. By contrast, *T. triandra* and *H. contortus* are more widely distributed across tablelands and valleys and are able to tolerate a broader range of climate conditions, possibly because they senesce aboveground structures during the cool dry season, hence avoiding the most stressful parts of the year. Nevertheless, although grasses are able to avoid harsh non-growing seasons, they may still develop unique ecotypes adapted to climatic differences during the growing season, as demonstrated by the haplotype structuring in this study. Thus, isolation by environment (IBE) may result in quite different spatial genetic structure across the YGP for herbs versus woody trees, as the latter must support perennial aboveground structures through the cold or hot dry seasons, which the former can avoid.

Our results clearly pointed towards the connection between climatic factors and phylogeographic patterns in *T. triandra and H. contortus*. This echoed recent evidence from studies of the nuclear genome of *T. triandra* populations in Australia that showed strong associations between gene pools and climate that were indicative of local adaptations (Ahrens et al., 2020). Studies also discovered an association between polyploidy and harsh environments in *T. triandra*, suggesting that polyploidy could increase reproductive flexibility and confer advantage in populations under stress (Godfree et al., 2017; Ahrens et al., 2020). Such autopolyploidy may lead to distinctive reproductive strategies, the development of spatial structure and reproductive barriers, and subsequently speciation (see Oberprieler et al., 2018). As our study did not examine the cytotype distribution of *T. triandra and H. contortus* in the YGP, it remains to be tested whether climate-driven polyploidy contribute to the observed genetic structure. This is clearly an interesting opportunity for future work to elucidate on the ploidy–environment interactions in the YGP.

4.4. Using phylogeography to unearth the history of savannas in Asia

The phylogeography method we adopted has been used by others to confirm the extent and antiquity of open habitats in Asia, notably by Agarwal and Ramakrishnan (2017) who studied the distribution and antiquity of lizards dependent on open habitats in South Asia, and by Zhang et al. (2011) who studied the population differentiation of YGP valley endemic tree *Terminalia franchettii*. By focusing on two dominant C_4 grass species, we provide direct empirical evidence on the phylogeographic patterns of grassy biomes, as opposed to an indirect assessment using vertebrate or woody species adapted to drier environments. Our findings prompt further investigation into the biogeographic history of grassy biomes in Asia using grasses themselves (Dunning et al., 2017). At the continental level, full genus and subfamily comparisons such as those focussed on Andropogonae may lead to insights as to the extent and age of grassy communities in Asia (e.g. Welker et al., 2020), as has been demonstrated in other areas where grassy communities were thought to be secondary, such as the grassy biomes of Madagascar (e.g. Hackel et al., 2018). Whereas those types of analyses will allow dating the evolution of grassy biomes in deep time, further extensive population genetics analyses of widely spread species such as *T. triandra* and *H. contortus* (Arthan et al., 2021) may be more suited for understanding the spatial extent of grassy biomes in Asia, as elsewhere.

Incidentally, our data suggest that *T. triandra* migrated into the YGP whereas *H. contortus* may have evolved in the YGP and several radiations of the species out of the region have occurred. We conclude this because our *T. triandra* samples collected in the YGP are nested as a clade within the wider clade of *T. triandra* sampled worldwide that we included in the phylogeny; conversely, all *H. contortus* samples taken outside the YGP lie within the clade of *H. contortus* samples we collected across YGP. Our *H. contortus* samples therefore push the emergence of the species several million years earlier than previous estimates (Arthan et al., 2021; Welker et al., 2020).

4.5. Implications for conservation in the YGP

Grassy biome physiognomy is common across southwest China and much of seasonally-dry tropical Asia (Ratnam et al., 2016). Yet most of these landscapes were until very recently (Su et al., 2020) designated as forest ecoregions (Dinerstein et al., 2017), and grassy biomes have received little protection, even though it is clear that numerous endemic C_4 grass species occur in these systems and depend on them (Ratnam et al., 2016). At present in Yunnan Province (where most of the drier part of the YGP is found), conservation is largely focussed on protecting the Hengduan Mountains Biodiversity Hotspot and different forest types found throughout the province (Zhao and Gong, 2015) and only one nature reserve has been specifically gazetted to protect Yuanjiang Valley savanna (Zhao et al., 2019). However, our study has demonstrated that both C_4 grass species we examined possess unique haplotypes on the cooler, wetter tablelands that have been present before humans are thought to have used fire in Asia, and therefore likely indicate the long-term presence of authentic grassy biome communities on the tablelands of the YGP. None of these areas have been designated for conservation of grassy biomes. Our work points to the urgent need to identify areas of conservation value for grassy biomes on the tablelands of the Yunnan-Guizhou Plateau.

CRediT authorship contribution statement

KWT and AKSW conceived and designed the study. YYC performed the data collection, sampling, DNA sequencing, and conducted the analyses, with assistance from KWT and AKSW. RSL produced the maps for the distribution of the species and the climate data. KWT provided funding. All four authors contributed to editing and completing the manuscript.

Declaration of Competing Interest

The authors declare that they have no known competing financial interests or personal relationships that could have appeared to influence the work reported in this paper.

Data accessibility

All relevant data collected in this manuscript is presented in the electronic Supplementary Material. The cpDNA sequences reported in this study can be downloaded from the dryad repository at doi:10.5061/dryad.ffbg79cw1. https://datadryad.org/stash/share/yfyDnX5_P095nGSaeLiIMihA13KV7xPER5C9PGw5yDI

Acknowledgements

This research was supported by a joint National Natural Science Foundation of China-Yunnan Government research grant to KWT (U1502264). AKSW is supported by the Guangxi University Start-up Fund, the Guangxi Provincial 100 Talent Grant from the Guangxi Department of Science and Technology, and the Research Fund for International Young Scientists under the International (Regional) Cooperation and Exchange Program from the National Natural Science Foundation of China (31850410481). RSL is supported by CAS-TWAS President's Fellowship for International Doctoral Students (Grant 2016CTF096). The authors thank Lu Yun, Hu Jirong and Zhang Xueqiao for field material sampling. We also thank Yang Jianhui and Mei Yingyi for raw data collection, and Dr Joeri Strijk for advice on the phylogenetic analysis.

Appendix A. Supporting information

Supplementary data associated with this article can be found in the online version at doi:10.1016/j.gecco.2021.e01835.

References

Agarwal, I., Ramakrishnan, U., 2017. A phylogeny of open-habitat lizards (Squamata: Lacertidae: *Ophisops*) supports the antiquity of Indian grassy biomes. J. Biogeogr. 44, 2021–2032. https://doi.org/10.1111/jbi.12999.

Ahrens, C.W., James, E.A., Miller, A.D., Scott, F., Aitken, N.C., Jones, A.W., Rymer, P.D., 2020. Spatial, climate and ploidy factors drive genomic diversity and resilience in the widespread grass. Themeda triandra. Mol. Ecol. 29 (20), 3872–3888.

Arthan, W., Dunning, L.T., Besbard, G., Manzi, S., Kellogg, E.A., Hackel, J., Vorontsova, M.S., 2021. Complex evolutionary history of two ecologically significant grass genera, *Themeda* and *Heteropogon* (Poaceae: Panicoideae: Andropogoneae). Bot. J. Linn. Soc. 196, 437–455. https://doi.org/10.1093/botlinnean/boab008.

Beierkuhnlein, C., Thiel, D., Jentsch, A., Willner, E., Kreyling, J., 2011. Ecotypes of European grass species respond differently to warming and extreme drought. J. Ecol. 99 (3), 703–713. https://doi.org/10.1111/j.1365-2745.2011.01809.x.

Biasatti, D., Wang, Y., F, G., Xu, Y., Flynn, L., 2012. Paleoecologies and paleoclimates of late cenozoic mammals from Southwest China: evidence from stable carbon and oxygen isotopes. J. Asian Earth Sci. 44, 48–61. https://doi.org/10.1016/j.jseaes.2011.04.013.

Bond, W.J., Stevens, N., Midgley, G.F., Lehmann, C.E.R., 2019. The trouble with trees: afforestation plans for Africa. Trends Ecol. Evol. 34 (11), 963–965. https://doi.org/10.1016/j.tree.2019.08.003.

Bond, W.J., Woodward, F.I., Midgley, G.F., 2005. The global distribution of ecosystems in a world without fire. New Phytol. 165 (2), 525–538. https://doi.org/10.1111/j.1469-8137.2004.01252.x.

Charles-Dominique, T., Midgley, G.F., Tomlinson, K.W., Bond, W.J., 2018. Steal the light: shade vs fire adapted vegetation in forest-savanna mosaics. New Phytol. 218 (4), 1419–1429. https://doi.org/10.1111/nph.15117.
Christin, P.A., Spriggs, E., Osborne, C.P., Stromberg, C.A.E., Salamin, N., Edwards, E.J., 2014. Molecular dating, evolutionary rates, and the age of the grasses. Syst. Biol. 63 (2), 153–165. https://doi.org/10.1093/sysbio/syt072.
Darriba, D., Taboada, G.L., Doallo, R., Posada, D., 2012. jModelTest 2: more models, new heuristics and parallel computing. Nat. Methods 9 (8), 772. https://doi.org/10.1038/nmeth.2109.
Dinerstein, E., Olson, D., Joshi, A., Vynne, C., Burgess, N.D., Wikramanayake, E., Saleem, M., 2017. An ecoregion-based approach to protecting half the terrestrial realm. BioScience 67 (6), 534–545. https://doi.org/10.1093/biosci/bix014.
Downing, B.H., Groves, R.H., 1985. Growth and development of four *Themeda triandra* populations from southern Africa in response to temperature. S. Afr. J. Bot. 51, 350–354.
Drummond, A.J., Rambaut, A., 2007. BEAST: Bayesian evolutionary analysis by sampling trees. BMC Evol. Biol. 7, 214. https://doi.org/10.1186/1471-2148-7-214.
Du, F.K., Hou, M., Wang, W.T., Mao, K.S., Hampe, A., 2017. Phylogeography of *Quercus aquifolioides* provides novel insights into the Neogene history of a major global hotspot of plant diversity in south-west China. J. Biogeogr. 44 (2), 294–307. https://doi.org/10.1111/jbi.12836.
Dunning, L.T., Liabot, A., Olofsson, J.K., Smith, E.K., Vorontsova, M.S., Besnard, G., Lehmann, C.E.R., 2017. The recent and rapid spread of *Themeda triandra*. Bot. Lett. 164 (4), 327–337. https://doi.org/10.1080/23818107.2017.1391120.
Godfree, R.C., Marshall, D.J., Young, A.G., Miller, C.H., Mathews, S., 2017. Empirical evidence of fixed and homeostatic patterns of polyploid advantage in a keystone grass exposed to drought and heat stress. R. Soc. Open Sci. 4 (11), 170934.
Gowlett, J.A.J., 2016. The discovery of fire by humans: a long and convoluted process. Philos. Trans. R. Soc. Lond. Ser. B Biol. Sci. 371 (20150164) https://doi.org/10.1098/rstb.2015.0164.
Hackel, J., Vorontsova, M.S., Nanjarisoa, O.P., Hall, R.C., Razanatsoa, J., Malakasi, P., Besnard, G., 2018. Grass diversification in Madagascar: in situ radiation of two large C3 shade clades and support for a Miocene to Pliocene origin of C4 grassy biomes. J. Biogeogr. 45 (4), 750–761. https://doi.org/10.1111/jbi.13147.
Huang, Y.J., Jia, L.B., Wang, Q., Mosbrugger, V., Utescher, T., Su, T., Zhou, Z.K., 2016. Cenozoic plant diversity of Yunnan: a review. Plant Divers. 38 (006), 271–282. https://doi.org/10.1016/j.pld.2016.11.004.
Jiang, X.L., An, M., Zheng, S.S., Deng, M., Su, Z.H., 2017. Geographical isolation and environmental heterogeneity contribute to the spatial genetic patterns of *Quercus kerrii* (Fagaceae). Heredity 120, 219–233. https://doi.org/10.1038/s41437-017-0012-7.
Jin, Z.Z., Ou, X.K., 2000. Yuanjiang, Nujiang, Jinshajiang, Lancangjiang: Vegetation of Dry-Hot Valley. Yunnan University Press, Kunming, China.
Ju, M.M., Fu, Y., Zhao, G.F., He, C.Z., Li, Z.H., Tian, B., 2018. Effects of the Tanaka Line on the genetic structure of *Bombax ceiba* (Malvaceae) in dry-hot valley areas of southwest China. Ecol. Evol. 3, 1–10. https://doi.org/10.1002/ece3.3888.
Karger, D.N., Conrad, O., Böhner, J., Kawohl, T., Kreft, H., Soria-Auza, R.W., Kessler, M., 2017a. Climatologies at high resolution for the earth's land surface areas! Abstract. Sci. Data 4, 170122. https://doi.org/10.1038/sdata.2017.122.
Karger, D.N., Conrad, O., Böhner, J., Kawohl, T., Kreft, H., Soria-Auza, R.W., Kessler, M., 2017b. Data from: climatologies at high resolution for the earth's land surface areas. Dryad Digit. Repos. https://doi.org/10.5061/dryad.kd1d4.
Kuhle, M., 2011. Last glacial maximum glaciation (LGM/LGP) in high Asia (Tibet and surrounding mountains). In: Singh, V.P., Singh, P., Haritashya, U.K. (Eds.), Encyclopedia of Snow, Ice and Glaciers. Encyclopedia of Earth Sciences Series. Springer, Dordrecht. https://doi.org/10.1007/978-90-481-2642-2_325.
Koressaar, T., Remm, M., 2007. Enhancements and modifications of primer design program Primer3. Bioinformatics 23, 1289–1291.
Kumar, S., Stecher, G., Tamura, K., 2016. MEGA7: molecular evolutionary genetics analysis version 7.0 for bigger datasets. Mol. Biol. Evol. 33 (7), 1870–1874. https://doi.org/10.1093/molbev/msw054.
Lehmann, C.E.R., Anderson, T.M., Sankaran, M., Higgins, S.I., Archibald, S., Hoffmann, W.A., Bond, W.J., 2014. Savanna vegetation-fire-climate relationships differ among continents. Science 343, 548–552. https://doi.org/10.1126/science.1247355.
Leigh, J.W., Bryant, D., 2015. POPART: full-feature software for haplotype network construction. Methods Ecol. Evol. 6, 1110–1116. https://doi.org/10.1111/2041-210X.12410.
Li, H.M., Zuo, X.X., Kang, L.H., Ren, L.L., Liu, F.W., Liu, H.G., Dong, G.H., 2016. Prehistoric agriculture development in the Yunnan-Guizhou Plateau, southwest China: archaeobotanical evidence. Sci. China Earth Sci. 59 (8), 1562–1573. https://doi.org/10.1007/s11430-016-5292-x.
Librado, P., Rozas, J., 2009. DnaSP v5: a software for comprehensive analysis of DNA polymorphism data. Bioinformatics 25 (11), 1451–1452. https://doi.org/10.1093/bioinformatics/btp187.
Liu, Y.P., Ren, Z.M., Harris, A., Peterson, P.M., Wen, J., Su, X., 2018. Phylogeography of *Orinus* (Poaceae), a dominant grass genus on the Qinghai-Tibet Plateau. Bot. J. Linn. Soc. 186 (2), 202–223. https://doi.org/10.1093/botlinnean/box091.
Ma, T., Zheng, Z., Man, M.L., Dong, Y.X., Li, J., Huang, K.Y., 2018. Holocene fire and forest histories in relation to climate change and agriculture development in southeastern China. Quat. Int. 488, 30–40. https://doi.org/10.1016/j.quaint.2017.07.035.
Malyshev, A.V., Henry, H.A.L., Kreyling, J., 2014. Relative effects of temperature vs. photoperiod on growth and cold acclimation of northern and southern ecotypes of the grass *Arrhenatherum elatius*. Environ. Exp. Bot. 106, 189–196. https://doi.org/10.1016/j.envexpbot.2014.02.007.
Metcalfe, 2017. Tectonic evolution of Sundaland. Bull. Geol. Soc. Malays. 63, 27–60. https://doi.org/10.7186/bgsm63201702.
Oberprieler, C., Konowalik, K., Fackelmann, A., Vogt, R., 2018. Polyploid speciation across a suture zone: phylogeography and species delimitation in S French Leucanthemum Mill. representatives (Compositae–Anthemideae). Plant Syst. Evol. 304 (9), 1141–1155.
Origin2019, 2019. version 9.6.0.37. OriginLab Corporation, Northampton, MA, USA.
Parks, D.H., Porter, M., Churcher, S., Wang, S., Blouin, C., Whalley, J., Beiko, R.G., 2009. GenGIS: a geospatial information system for genomic data. Genome Res. 19 (10), 1896–1904. https://doi.org/10.1101/gr.095612.109.
Peakall, R., Smouse, P.E., 2012. GenAlEx 6.5: genetic analysis in Excel. Population genetic software for teaching and research–an update. Bioinformatics 28 (19), 2537–2539. https://doi.org/10.1093/bioinformatics/bts460.
Qian, F., Li, Q., Wu, P., Yuan, S., Xing, R., Chen, H., Zhang, H., 1991. Lower Pleistocene, Yuanmou Formation: Quaternary Geology and Paleoanthropology of Yuanmou, Yunnan, China. Science Press, Beijing.
Ratnam, J., Bond, W.J., Fensham, R.J., Hoffmann, W.A., Archibald, S., Lehmann, C.E.R., Sankaran, M., 2011. When is a 'forest' a savanna, and why does it matter? Glob. Ecol. Biogeogr. 20, 653–660. https://doi.org/10.1111/j.1466-8238.2010.00634.x.
Ratnam, J., Tomlinson, K.W., Rasquinha, D.N., Sankaran, M., 2016. Savannahs of Asia: antiquity, biogeography, and an uncertain future. Philos. Trans. R. Soc. Lond. Ser. B Biol. Sci. 371 (1703) https://doi.org/10.1098/rstb.2015.0305.
R Core Team, 2020. R: A Language and Environment for Statistical Computing. R Foundation for Statistical Computing, Vienna, Austria. ⟨https://www.R-project.org/⟩.
Reynolds, C., Cumming, G.S., 2016. Seed dispersal by waterbirds in southern Africa: comparing the roles of ectozoochory and endozoochory. Freshw. Biol. 61 (4), 349–361. https://doi.org/10.1111/fwb.12709.
Ripley, B., Visser, V., Christin, P.-A., Archibald, S., Osborne, C., Martin, T., Osborne, C., 2015. Fire ecology of C_3 and C_4 grasses depends on evolutionary history and frequency of burning but not photosynthetic type. Ecology 96, 2679–2691.
Ronquist, F., Teslenko, M., van der Mark, P., Ayres, D.L., Darling, A., Höhna, S., Larget, B., Liu, L., Suchard, M.A., Huelsenbeck, J.P., 2012. MRBAYES 3.2: efficient Bayesian phylogenetic inference and model selection across a large model space. Syst. Biol. 61, 539–542.
Rudov, A., Mashkour, M., Djamali, M., Akhani, H., 2020. A review of C_4 plants in southwest Asia: an ecological, geographical and taxonomical analysis of a region with high diversity of C_4 eudicots. Front. Plant Sci. 11, 546518 https://doi.org/10.3389/fpls.2020.546518.
Sage, R.F., 2017. A portrait of the C_4 photosynthetic family on the 50th anniversary of its discovery: species number, evolutionary lineages, and Hall of Fame. J. Exp. Bot. 68, e11–e28. https://doi.org/10.1093/jxb/erx005.
Shang, L., Li, L.F., Song, Z.P., Wang, Y., Yang, J., C, W.C., Li, B., 2019. High genetic diversity with weak phylogeographic structure of the invasive *Spartina alterniflora* (Poaceae) in China. Front. Plant Sci. 10, 1467. https://doi.org/10.3389/fpls.2019.01467.

Shen, G., Gao, X., Gao, B., Granger, D.E., 2009. Age of Zhoukoudian *Homo erectus* determined with $^{26}Al/^{10}Be$ burial dating. Nature 458 (7235), 198–200. https://doi.org/10.1038/nature07741.

Shi, H.Y., Chen, J., 2018. Characteristics of climate change and its relationship with land use/cover change in Yunnan Province, China. Int. J. Clim. 38 https://doi.org/10.1002/joc.5404.

Shi, Z.G., Sha, Y.Y., Liu, X.D., 2017. Effect of Yunnan-Guizhou topography at the southeastern Tibetan Plateau on the Indian monsoon. J. Clim. 30, 1259–1272. https://doi.org/10.1175/JCLI-D-16-0105.1.

Schubert, M., Marcussen, T., Meseguer, A.S., Fjellheim, S., 2019. The grass subfamily Pooideae: Cretaceous-Palaeocene origin and climate-driven Cenozoic diversification. Glob. Ecol. Biogeogr. 28, 1168–1182.

Snyman, H.A., Ingram, L.J., Kirkman, K.P., 2013. *Themeda triandra*: a keystone grass species. Afr. J. Range Forage Sci. 30 (3), 99–125. https://doi.org/10.2989/10220119.2013.831375.

Spriggs, E.L., Christin, P.-A., Edwards, E.J., 2014. C_4 photosynthesis promoted species diversification during the Miocene grassland expansion. PLoS One 9 (5), 97722. https://doi.org/10.1371/journal.pone.0097722.

Stott, P., 1988. The forest as phoenix: towards a biogeography of fire in mainland South East Asia. Geogr. J. 154, 337–350. https://doi.org/10.2307/634607.

Stucky, B.J., 2012. SeqTrace: a graphical tool for rapidly processing DNA sequencing chromatograms. J. Biomol. Tech. 23 (3), 90–93. https://doi.org/10.7171/jbt.12-2303-004.

Su, Y.J., Guo, Q.H., Hu, T.Y., Guan, H.C., Ma, K.P., 2020. An updated vegetation map of China (1:1000000). Sci. Bull. 65, 1126–1135. https://doi.org/10.1016/j.scib.2020.04.004.

Trabucco, A., Zomer, R.J., 2018. Global Aridity Index and Potential Evapo-Transpiratuin(ETO) Climate Database. (Published online). ⟨http://cgiarcsi.community⟩.

Untergasser, A., Cutcutache, I., Koressaar, T., Ye, J., Faircloth, B.C., Remm, M., Rozen, S.G., 2012. Primer3 - new capabilities and interfaces. Nucleic Acids Res. 40, e115.

Vandenberghe, J., French, H.M., Gorbunov, A., Marchenko, S., Velichko, A.A., Jin, H., Cui, Z., Zhang, T., Wan, X., 2014. The Last Permafrost Maximum (LPM) map of the Northern Hemisphere: permafrost extent and mean annual air temperatures, 25–17 ka BP. Boreas 43, 652–666. https://doi.org/10.1111/bor.12070. ISSN 0300-9483.

Vicentini, A., Barber, J.C., Aliscioni, S.S., Giussani, L.M., Kellogg, E.A., 2008. The age of the grasses and clusters of origins of C4 photosynthesis. Glob. Chang. Biol. 14, 2963–2977.

Welker, C.A.D., McKain, M.R., Estep, M.C., Pasquet, R.S., Chipabika, G., Pallangyo, B., Kellogg, E.A., 2020. Phylogenomics enables biogeographic analysis and a new subtribal classification of Andropogoneae (Poaceae—Panicoideae). J. Syst. Evol. 58, 1003–1030. https://doi.org/10.1111/jse.12691.

Wu, F., Gao, S., Tang, F., Meng, Q., An, C., 2019. A late Miocene-early Pleistocene palynological record from the Yunnan Plateau and its climatic and tectonic implications for the Eryuan Basin, China. Palaeogeogr. Palaeoclimatol. Palaeoecol. 530, 190–199. https://doi.org/10.1016/j.palaeo.2019.05.037.

Wu, L.Q., 2004. Rivers and water resources of Yunnan province. Yangtze River 35 (5), 48–50.

Yan, H.D., Zhang, X.Q., Fu, C., Huang, L.K., Yin, G., Nie, G., Liu, W., 2015. Chloroplast DNA variation and genetic structure of *Miscanthus sinensis* in southwest China. Biochem. Syst. Ecol. 58, 132–138. https://doi.org/10.1016/j.bse.2014.11.007.

Yang, Y.T., Hou, X.Y., Wei, Z.W., Qiao, Z.H., Chang, C., Ren, W.B., Wu, Z.N., 2018. Screening and genetic diversity analysis of chloroplast non-coding regions in *Leymus chinensis*. Acta Pratacult. Sin. 27 (10), 147–157. https://doi.org/10.11686/cyxb2018022.

Yao, Y.F., Bruch, A.A., Cheng, Y.M., Mosbrugger, V., Wang, Y.F., Li, C.S., 2012. Monsoon versus uplift in southwestern China–Late Pliocene climate in Yuanmou Basin, Yunnan. PLoS One 7 (5), 37760. https://doi.org/10.1371/journal.pone.0037760.

Zhang, T.C., Comes, H.P., Sun, H., 2011. Chloroplast phylogeography of *Terminalia franchetii* (Combretaceae) from the eastern Sino-Himalayan region and its correlation with historical river capture events. Mol. Phylogenet. Evol. 60 (1), 1–12. https://doi.org/10.1016/j.ympev.2011.04.009.

Zhang, W.X., Ming, Q.Z., Shi, Z.T., Chen, G.J., Niu, J., Lei, G.L., Zhang, H.C., 2014. Lake sediment records on climate change and human activities in the Xingyun Lake Catchment, SW China. PLoS One 9 (7), 102167.

Zhao, H.W., Wu, R.D., Long, Y.C., Hu, J.M., Yang, F.L., Jin, T., Guo, Y., 2019. Individual-level performance of nature reserves in forest protection and the effects of management level and establishment age. Biol. Conserv. 233, 23–30. https://doi.org/10.1016/j.biocon.2019.02.024.

Zhao, Y.J., Gong, X., 2015. Genetic divergence and phylogeographic history of two closely related species (*Leucomeris decora* and *Nouelia insignis*) across the 'Tanaka Line' in Southwest China. BMC Evol. Biol. 15 (134), 1–13. https://doi.org/10.1186/s12862-015-0374-5.

Zhu, Z.Y., Dennell, R., Huang, W.W., Wu, Y., Qiu, S.F., Yang, S.X., Han, J.W., 2018. Hominin occupation of the Chinese Loess Plateau since about 2.1 million years ago. Nature 559, 608–612. https://doi.org/10.1038/s41586-018-0299-4.